Cellular/Molecular

Efficient T-Cell Surveillance of the CNS Requires Expression of the CXC Chemokine Receptor 3

Jeanette Erbo Christensen,[1] Anneline Nansen,[1] Torben Moos,[2] Bao Lu,[3] Craig Gerard,[3] Jan Pravsgaard Christensen,[1] and Allan Randrup Thomsen[1]

[1]Institute of Medical Microbiology and Immunology and [2]Department of Medical Anatomy, University of Copenhagen, Copenhagen, Denmark, and [3]Ina Sue Perlmutter Laboratory, Children's Hospital and Harvard Medical School, Boston, Massachusetts 02115

T-cells play an important role in controlling viral infections inside the CNS. To study the role of the chemokine receptor CXCR3 in the migration and positioning of virus-specific effector T-cells within the brain, CXCR3-deficient mice were infected intracerebrally with lymphocytic choriomeningitis virus (LCMV). Analysis of the induction phase of the antiviral $CD8^+$ T-cell response did not reveal any immune defects in CXCR3-deficient mice. Yet, when mice were challenged with LCMV intracerebrally, most CXCR3-deficient mice survived the infection, whereas wild-type mice invariably died from $CD8^+$ T-cell-mediated immunopathology. Quantitative analysis of the cellular infiltrate in CSF of infected mice revealed modest, if any, decrease in the number of mononuclear cells recruited to the meninges in the absence of CXCR3. However, immunohistological analysis disclosed a striking impairment of $CD8^+$ T-cells from CXCR3-deficient mice to migrate from the meninges into the outer layers of the brain parenchyma despite similar localization of virus-infected target cells. Reconstitution of CXCR3-deficient mice with wild-type $CD8^+$ T-cells completely restored susceptibility to LCMV-induced meningitis. Thus, taken together, our results strongly point to a critical role for CXCR3 in the positioning of effector T-cells at sites of viral inflammation in the brain.

Key words: **viral infection; immunopathology; chemokines; CXCR3; T-cells; knock-out mice**

Introduction

Under normal conditions, lymphocyte traffic into the CNS is low, most likely to reduce the risk for debilitating immunopathology (Hickey, 2001; Lowenstein, 2002). However, during infection and inflammatory diseases of the CNS such as multiple sclerosis (MS) and experimental autoimmune encephalomyelitis (EAE), large numbers of circulating lymphocytes readily gain access to the CNS.

Over the last decade, chemokines have emerged as pivotal players in the pathogenesis of immune-mediated inflammatory diseases of the CNS (Ransohoff, 1999; Zhang et al., 2000; Trebst and Ransohoff, 2001). Thus, chemokines are thought to play an important role in leukocyte extravasation as well as subsequent migration of inflammatory cells deeper within the CNS (Karpus and Ransohoff, 1998).

One chemokine that has been suggested to be critically involved in the accumulation of leukocytes inside the CNS is CXCL10 [interferon (IFN)-γ-inducible protein of 10 kDa (IP-10)]. CXCL10 has been found in the CSF of patients with viral meningitis (Lahrtz et al., 1997; Kolb et al., 1999) and MS (Sorensen et al., 1999; Franciotta et al., 2001). Furthermore, cells positive for CXCL10 has been detected in large numbers in active MS and EAE lesions (Balashov et al., 1999; Sorensen et al., 1999; Simpson et al., 2000). Experimentally, a role for CXCL10 has been supported by studies both in the EAE model and in a murine viral hepatitis model with both acute and chronic stages of CNS inflammation (Liu et al., 2000, 2001; Fife et al., 2001; Dufour et al., 2002).

CXCL10 is structurally and functionally related to CXCL9 (monokine induced by IFN-γ) and CXCL11 (IFN-inducible T-cell α-chemoattractant). The corresponding receptor for this group of chemokines is CXCR3 (Loetscher et al., 1996; Weng et al., 1998), which has been found on the majority of infiltrating T-cells in MS lesions (Balashov et al., 1999; Sorensen et al., 1999, 2002; Simpson et al., 2000). The above results, therefore, suggest that interactions between CXCR3 and CXCL10 might regulate trafficking of antigen-primed T-cells to sites of inflammation inside the CNS.

The primary aim of this study was to obtain a better understanding of the role of CXCR3 in regulating antiviral T-cell-mediated immune surveillance of the CNS. For this purpose, CXCR3-deficient mice were infected intracerebrally with lymphocytic choriomeningitis virus (LCMV). LCMV is a noncytolytic virus. However, intracerebral inoculation of LCMV leads to infection of the meninges and choroid plexus, and in immunocompetent mice, the result is a severe $CD8^+$ T-cell-mediated meningitis that normally kills animals within 7–10 d

Received Jan. 13, 2004; revised April 2, 2004; accepted April 5, 2004.

This work was supported in part by the Danish Medical Research Council, the Lundbeck Foundation, the Leo Pharma Research Foundation, and the Novo Nordisk Foundation. J.E.C. was a recipient of a Ph.D. scholarship from the Faculty of Health Science, University of Copenhagen, and J.P.C. was the recipient of a postdoctoral fellowship from the Alfred Benzon Foundation.

Correspondence should be addressed to Dr. Allan Randrup Thomsen, Institute of Medical Microbiology and Immunology, University of Copenhagen, The Panum Institute, 3C Blegdamsvej, DK-2200 Copenhagen N, Denmark. E-mail: A.R.Thomsen@immi.ku.dk.

DOI:10.1523/JNEUROSCI.0123-04.2004

 0270-6474/04/244849-10$15.00/0

post infection (dpi) (Ceredig et al., 1987; Doherty et al., 1990; Christensen et al., 1995). Supporting a role for chemokines in LCMV-induced immunopathology, mRNA for both CXCL10 and CXCR3 has been found in the brains of intracerebrally infected mice (Asensio and Campbell, 1997; Nansen et al., 2000; Lindow et al., 2003).

In the present study, we found that, unlike wild-type mice, intracerebrally infected CXCR3-deficient mice do not succumb to virus-induced $CD8^+$ T-cell-mediated immunopathology and that this primarily reflects a failure of CXCR3-deficient $CD8^+$ T-cells to migrate from the meninges and into the outer layers of the brain parenchyma.

Materials and Methods

Mice. The generation of CXCR3-deficient mice has been described before (Hancock et al., 2000). The animals used in these experiments were the progeny of breeder pairs kept at the Panum Institute, University of Copenhagen. Wild-type (WT) C57BL/6 mice were purchased from Taconic M & B (Ry, Denmark), and they were always allowed to rest for at least one week before entering into experiments; by that time, the animals were ~7–9 weeks old. Transgenic C57BL/6 mice (TCR318) expressing a T-cell receptor (TCR) specific for LCMV (gp33-41; immunodominant epitope in $H\text{-}2^b$ mice) on ~60% of their $CD8^+$ T-cells were bred locally from breeder pairs originally provided by H. Pircher (Zurich, Switzerland) and R. M. Zinkernagel (Zurich, Switzerland) (Pircher et al., 1989). Animals were housed under controlled (specific pathogen free) conditions that included the testing of sentinels for unwanted infections according to Federation of European Laboratory Animal Science Association standards; no irrelevant infections were detected. Female mice were used in most experiments, but when both sexes were used, no gender effect was observed.

Virus infection. Mice were infected intracerebrally with a virus dose of 10^3 LD_{50} (~200 pfu) of LCMV Traub in a volume of 0.03 ml. Intracerebral infection induces a fatal $CD8^+$ T-cell-mediated meningitis from which immunocompetent mice die on 7–10 dpi (Christensen et al., 1994).

Survival study. Mortality was used to evaluate the clinical severity of acute LCMV-induced meningitis. Mice were checked twice daily for a minimum of 2 weeks after intracerebral inoculation; deaths occurring <5 d after infection were excluded from analysis.

Organ virus titers. To determine virus titers in organs, these were first homogenized in PBS to yield 10% (v/w) organ suspensions, and serial 10-fold dilutions were prepared. Each dilution was then plated in duplicate on MC57G cells. Forty-eight hours after infection, infected cell clusters were detected using monoclonal rat anti-LCMV (VL-4) antibody, peroxidase-labeled goat anti-rat antibody, and o-phenylendiamin (substrate) (Battegay et al., 1991). The numbers of plaque-forming units were counted, and results were expressed as plaque-forming units per gram of tissue.

Cell preparations. Single-cell suspensions of spleen cells were obtained by pressing the organs through a fine steel mesh, and, when required, erythrocytes were lysed by 0.83% NH_4Cl treatment.

CSF cell count. CSF was obtained from the fourth ventricle of mice deeply anesthetized with ether and exsanguinated. The total number of inflammatory cells (background level in uninfected mice is <100 cells/μl) was determining by counting in hemocytometer, and phenotypic analysis was performed by flow cytometry (see below).

$CD8^+$ T-cell depletion of splenocytes. Single-cell suspension of spleen cells from TCR318 mice were incubated with anti-Ly 2.2 (Cedarlane Laboratories, Hornby, Canada) for 60 min at 4°C and washed. Cells were then incubated in a mixture of Low-Tox guinea pig and Low-Tox rabbit complement for 60 min at 37°C and washed; the efficiency of cell depletion was always validated by flow cytometric analysis (see below). Finally, 3×10^6 cells were transferred to each recipient.

Antibodies for flow cytometry. The following monoclonal antibodies were purchased from PharMingen (San Diego, CA) as rat anti-mouse antibody: phycoerythrin (PE)-, peridinin chlorophyll protein-, and Cychrome-conjugated anti-CD8; allophycocyanin-conjugated anti-CD4; FITC- and PE-conjugated anti-VLA-4 (CD49d); FITC-conjugated anti-CD44; FITC-conjugated anti-Mac-1 (CD11b); FITC-conjugated anti-L-selectin (CD62L); PE-conjugated anti-B220 (CD45R); PE-conjugated anti-IFN-γ; and PE-conjugated IgG_1 isotype standard. Rabbit anti-CXCR3 antibody and biotin-SP-conjugated goat anti-rabbit antibody were purchased from Zymed (San Francisco, CA). Streptavidin–Tricolor was purchased from Caltag (Burlingame, CA).

Flow cytometric analysis. Staining of cells for flow cytometry was performed according to standard laboratory procedure (Andersson et al., 1994; Andreasen et al., 1999). For enumeration of LCMV-specific $CD8^+$ T-cells, splenocytes were incubated *in vitro* for 5 hr at 37°C in 5% CO_2 with gp33-41 peptide (0.1 μg/ml) in the presence of monensin (3 μM; Sigma, St. Louis, MO) and murine recombinant interleukin (IL)-2 (10 U/well; R & D Systems Europe, Abingdon, UK). After incubation, cells were surface stained, washed and permeabilized using 0.5% saponin. Cells were then stained with anti-IFN-γ or IgG_1 isotype control for 20 min at 4°C. Samples were analyzed using a Becton Dickinson FACSCalibur, and at least 10^4 mononuclear cells were gated using a combination of low angle and side scatter to exclude dead cells and debris. Data analysis was conducted using Cell Quest (B&D Biosciences, San Jose, CA), and results are presented as dot plots.

Detection of mRNA in the brain. Brains from mice deeply anesthetized with ether and exsanguinated were immediately removed, snap frozen in liquid nitrogen, and stored in a liquid nitrogen freezer. Total RNA was extracted from homogenized brains by use of the RNeasy midi kit (Qiagen, Hilden, Germany). Transcription levels were studied using the RiboQuant multi-probe RNase protection assay (RPA) system (PharMingen) (Nansen et al., 2000, 2002). The following template sets (PharMingen) were used: T-cell marker mRNA (CD3ϵ, CD4, CD11b, CD8, F4/80), cytokine marker mRNA (IL-4, IL-5, IL-10, IL-13, IL-15, IL-9, IL-2, IL-6, IFN-γ) chemokine receptor marker mRNA (CCR1, CCR3, CCR4, CCR5, CCR2, CCR7, CCR8, CXCR3), and chemokine marker mRNA [XCL1 (Lymphotactin), CCL5 (RANTES), CCL11 (Eotaxin), CCL4 (macrophage inflammatory protein (MIP)-1β), CCL3 (MIP-1α), CXCL1–2 (MIP-2), CXCL10 (IP-10), CCL2 (MCP-1), and CCL1 (TCA-3)]. All sets of probes included templates for the housekeeping genes L-32 and glyceraldehyde-3-phosphate dehydrogenase to serve as loading controls. The RPA was performed according to the manufacturer's instructions. Briefly, [α-^{32}P] UTP-labeled antisense RNA transcript was generated from the template sets using T7 RNA polymerase. RNA from each sample was allowed to hybridize to the labeled probe for 16–20 hr at 56°C. Single-stranded RNA was digested with an RNase/T1 mixture, and the hybrids were analyzed on a denaturing urea-polyacrylamide gel. Protected fragments were visualized by autoradiography by placing dried gels on film (Biomax MS-1; Kodak, New Haven, CT) in cassettes with intensifying screens (Biomax MS; Kodak), which were then exposed at −80°C. For quantitative results, gels were subjected to PhosphorImager analysis (Amersham Biosciences, Piscataway, NJ), and the data were subsequently analyzed using ImageMaster TotalLab software (Amersham Biosciences).

Chemotaxis assay. Cell suspensions were prepared from spleens as described above and subsequently incubated for 1 hr in 5% CO_2 at 37°C, to compensate for any chemokine-induced downregulation or desensitization of relevant chemokine receptors. Migration assays were performed using Transwell chambers with culture inserts of 6.5 mm and 5 μm pore size (Corning Costar, Acton, MA). rmCXCL10 and rmCCL3 (R & D Systems) solutions at pretitrated optimal concentrations or assay medium alone were added to the lower chambers of the transwells. Then, filter inserts were placed in the wells, and a total of 1.5×10^6 splenocytes were added to the top chamber. After 3 hr in 5% CO_2 at 37°C, the cells in the lower chamber were quantified, and the results were presented as a percentage of input cell numbers. Additionally, the phenotypes of the transmigrated cells were analyzed using flow cytometry. All analyses were performed in triplicate.

Histology. WT and CXCR3-deficient mice were examined for the cerebral distribution of T-cells subsequent to an intracerebral LCMV challenge applied as described above. Surviving mice were examined at postinoculation time points 7 d (C57BL/6, $n = 5$; CXCR3 deficient, $n = 5$), 14 d (CXCR3 deficient, $n = 5$), and 21 d (CXCR3 deficient, $n = 3$). For

euthanasia, the mice were deeply anesthetized with tribromoethanol (Sigma) intraperitoneally and decapitated. Brains were dissected rapidly and frozen by applying to carbon dioxide snow. Subsequently, the brains were cut into serial, coronal 10 μm sections on a freezing microtome, mounted on gelatinized slides, and stored at −80°C for a maximum of 7 d before being reacted.

Immunohistochemistry. The cryostat sections were fixed for 2 min in acetone kept at −20°C and rapidly dried in a fume-hood. The sections were then washed three times for 5 min in 0.1 M PBS, pH 7,4 followed by incubation with 5% normal swine serum (X0901; Dako, Glostrup, Denmark) diluted in 1% BSA in PBS/0.3% Triton X-100 (BSA/TX100) to block nonspecific binding by the antibodies. Next, sections were incubated overnight at 4°C with monoclonal rat anti-mouse CD8a (550281; BD Biosciences) diluted 1:50 in BSA/TX100. Alternatively, monoclonal rat anti-mouse LCMV antibody (VL-4; kindly provided by R. M. Zinkernagel) (Battegay et al., 1991; Odermatt et al., 1991) diluted 1:100 was used to detect viral protein in the brain. The next day, specific binding by the antibody was detected using affinity purified, mouse absorbed biotinylated rabbit anti-rat IgG (BA-4001; Vector Laboratories, Burlingame, CA) diluted 1:100 for 30 min at room temperature, followed by incubation with HRP-conjugated streptavidin–biotin complex (Vectastain; Vector Laboratories) prepared at the manufacturer's recommended dilution. Finally, the sections were developed in DAB and 0.01% H202 in 0.05 M Tris buffer, pH 7.6 for 10 min. Between each step described above, the sections were washed three times for 5 min in PBS containing 0.25% BSA and 0.1% Triton X-100. The sections were coverslipped with DePeX (BDH Chemicals, Poole, UK). To evaluate the extent of nonspecific binding of the primary antibody in the immunohistochemical studies, the preincubation agent (swine serum and BSA) was substituted for the primary antibody step described above, and results were considered only if this control was negative.

Quantitative morphological analysis. Counts of CD8$^+$ T-cells were performed in sections using a standardized protocol for estimating cell density, which involved counting the number of CD8$^+$ T-cells in a 10 × 10 mm frame overlaying the forebrain area immediately lateral to the choroid plexus of the lateral ventricle at 250× magnification equivalent to an area of 150,000 μm^2. Three sections with an individual distance of ~300 μm were examined in brains of WT mice on 7 dpi ($n = 5$), and CXCR3-deficient mice on 7 dpi ($n = 5$) and 14 dpi ($n = 5$). Data were examined by ANOVA, and means were compared with the Student–Newman–Keuls test for differences between individual means. Evidence of a statistically significant difference between mean values was considered to be $p < 0.05$.

Virus-induced delayed-type hypersensitivity. LCMV-specific delayed-type hypersensitivity was assessed in mice infected locally in the right hind footpad with 200 pfu of LCMV in 0.03 ml. Footpad thickness was measured using a dial caliper (Mitutoyo, Tokyo, Japan), and virus-specific swelling was calculated as the difference in thickness of the infected right and the uninfected left hind foot (Thomsen and Marker, 1989).

Results

CXCR3 expression on primed CD8$^+$ T-cells

Transcripts for CXCR3 can be found in inflamed organs of immunocompetent mice infected with LCMV (Lindow et al., 2003). To study the expression of CXCR3 on virus-activated CD8$^+$ T-cells, WT mice were infected intracerebrally with LCMV, and 7 d later, CD8$^+$ T-cells from the spleen and from CSF were analyzed for CXCR3 expression using flow cytometry. For comparison, CD8$^+$ splenocytes from uninfected WT and CXCR3-deficient mice were also analyzed for CXCR3 expression (Fig. 1). Compared with cells from CXCR3-deficient mice, ~20% of CD8$^+$ T-cells from uninfected WT mice were positive for CXCR3 expression. This subset was nearly identical to the CD44^{high} subset of CD8$^+$ T-cells, indicating that CXCR3 is expressed on previously primed (effector/memory) CD8$^+$ T-cells. Consistent with this interpretation, the virus-induced increase in the frequency of activated CD44^{high}CD8$^+$ T-cells in WT mice led to a similar increase in the frequency of CXCR3$^+$ CD8$^+$ T-cells (→83%). In addition, nearly all (96%) CD8$^+$ T-cells harvested from the CSF of mice infected intracerebrally were CXCR3$^+$, suggesting that this receptor could be directly involved in the recruitment of recently activated CD8$^+$ T-cells to sites of inflammation within the CNS.

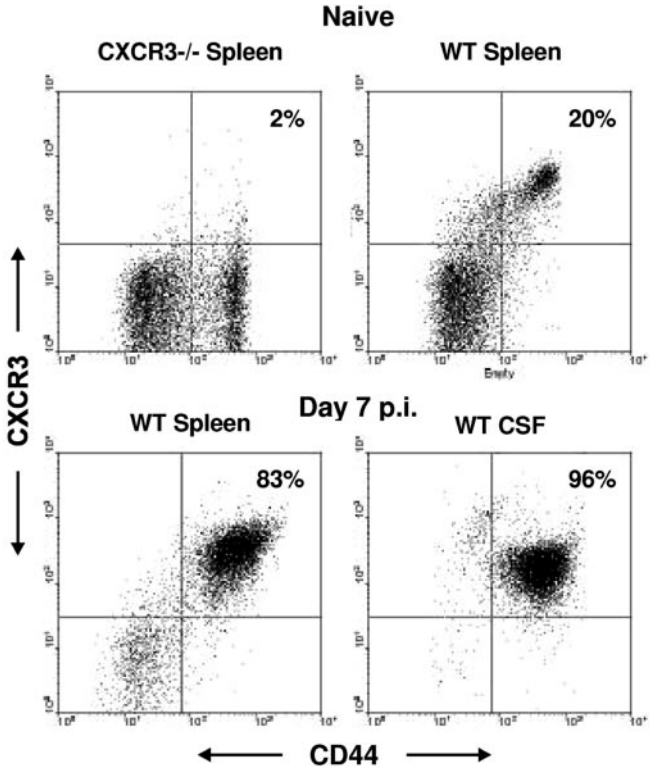

Figure 1. CXCR3 expression on CD8$^+$ T-cells as a function of their activation state. Splenocytes were taken from uninfected WT and CXCR3-deficient mice. In addition, splenocytes and CSF cells were harvested from WT mice infected intracerebrally with 10^3 LD_{50} of LCMV 7 d earlier. All cells were stained with anti-CD8, anti-CD44, and anti-CXCR3. Gates were set for CD8$^+$ cells; results are representative of more than five mice per group.

To more directly assess the potential of CXCR3 to play an active role in effector cell recruitment, we used a Transwell migration assay to evaluate chemokine-induced cell migration *in vitro*. Splenocytes from CXCR3-deficient and WT mice infected intracerebrally with LCMV 7 d earlier were used in the assay, and splenocytes from uninfected mice served as control. As chemoattractants, we used CXCL10 (IP-10/crg-2), and for a positive control, CCL3 (MIP-1α). Transcripts for both these ligands are rapidly upregulated in the brain of mice infected intracerebrally with LCMV (Asensio and Campbell, 1997; Nansen et al., 2000).

Confirming recent analysis (Frigerio et al., 2002; Lindow et al., 2003; Madsen et al., 2003), both CXCL10 and CCL3 acted as chemoattractants of splenocytes from LCMV-infected WT mice, and flow cytometric analysis revealed that the recruited cells were activated CD8$^+$ T-cells and cells with a low-angle/side scatter pattern consistent with that of mononuclear phagocytes, the two cell types known to dominate in the virus-induced inflammatory exudate (Ceredig et al., 1987; Christensen et al., 1995) (data not shown). In contrast, CCL3, but not CXCL10, induced the migration of cells from LCMV-infected CXCR3-deficient mice. Taken together, the above findings strongly indicate that virus-activated CD8$^+$ T-cells express functionally relevant CXCR3 receptors.

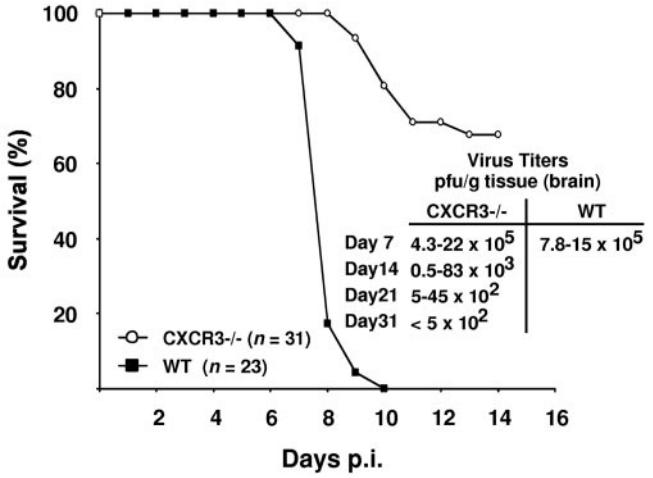

Figure 2. Lack of CXCR3 expression protects mice against a fatal outcome of LCMV-induced T-cell-mediated meningitis. WT and CXCR3-deficient mice were infected intracerebrally with 10^3 LD_{50} of LCMV, and mortality was registered ($n = 23–31$/group). Statistical evaluation was performed using the Mantel–Cox test: $p < 0.0001$. Brain virus titers of mice from parallel groups were determined and expressed as plaque-forming units per gram of organ ($n = 3–4$ mice/group).

CXCR3-deficient mice are less susceptible to LCMV-induced T-cell-mediated meningitis

Next, we wanted to determine whether lack of CXCR3 expression would influence effector T-cell recruitment to the virus-infected CNS. For this purpose, CXCR3-deficient mice and WT mice were again infected intracerebrally with LCMV, and the susceptibility to fatal meningitis was studied. As shown in Figure 2, all infected WT mice died from $CD8^+$ T-cell-mediated meningitis within 7–10 d of infection, whereas the majority of CXCR3-deficient mice survived the infection. This relative resistance to intracerebral infection did not reflect any difference in peak viral load because similar brain virus titers were measured on 7 dpi regardless of genotype ($p > 0.1$, Mann–Whitney rank sum test) (Fig. 2). Notably, despite the weakening of the immune attack with regard to induction of immunopathology, virus was eventually cleared from the brains of CXCR3-deficient mice (Fig. 2). Thus, by 1 month after infection, no virus was detected in any of the surviving mice.

Generation of activated $CD8^+$ T-cells is unimpaired in intracerebrally infected CXCR3-deficient mice

Because the reduced immunopathology in CXCR3-deficient mice could reflect an impaired antiviral $CD8^+$ T-cell response, we asked whether lack of CXCR3 expression would impair the expansion and differentiation of LCMV-activated $CD8^+$ T-cells in secondary lymphoid tissues. For this purpose, we studied the kinetics of effector cell generation by determining the total number of $CD8^+$ splenocytes with an activated (VLA-4^{high}L-selectin^{low}) phenotype as well as the number of splenic $CD8^+$ T-cells with specificity for an immunodominant major histocompatiblity complex class I-restricted LCMV-encoded epitope (gp 33-41). CXCR3-deficient mice and WT mice were infected intracerebrally with LCMV, and on the days leading up to the fatal inflammatory disease in WT mice (5–7 dpi), splenocytes were analyzed by flow cytometry. As shown in Fig. 3, similar splenic $CD8^+$ T-cell expansion was observed regardless of genotype, indicating that lack of CXCR3 expression did not impair the induction of the LCMV-specific $CD8^+$ T-cell response.

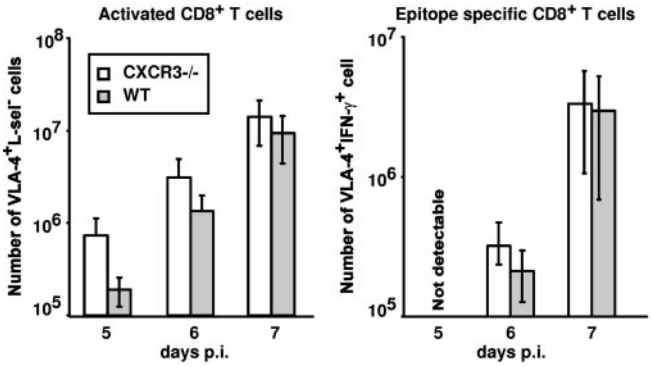

Figure 3. Unimpaired $CD8^+$ T-cell expansion in LCMV-infected CXCR3-deficient mice. Mice were infected intracerebrally with 10^3 LD_{50} of LCMV, and on 5–7 dpi, splenocytes were stained with anti-CD8, anti-VLA-4, and anti-L-selectin to determine the frequency of $CD8^+$ T-cells with an activated phenotype. Gates were set for $CD8^+$ T-cells, and the total number of VLA-4^{high}/I-sel^{low} cells/spleen is presented. To determine the frequency of virus-specific $CD8^+$ T-cells, cells were stained for intracellular IFN-γ after *in vitro* stimulation with LCMV gp33-41 peptide for 5 hr. Gates were set for $CD8^+$ T-cells, and the total number of VLA-4^{high}/IFN-γ^+ cells/spleen is presented. Averages ± SDs of four to eight mice per group are depicted.

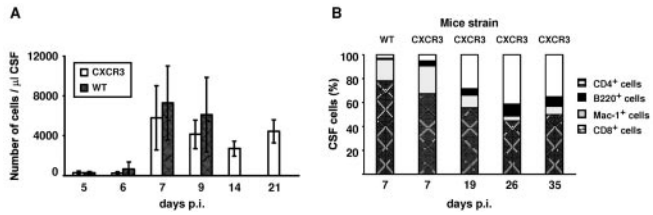

Figure 4. Leukocyte recruitment to the CSF is not impaired in virus-infected CXCR3-deficient mice. *A*, Kinetics of leukocyte recruitment to the CSF of LCMV-infected mice. CXCR3-deficient and WT mice were infected intracerebrally with 10^3 LD_{50} of LCMV, and on the indicated days, CSF was harvested and the number of exudate cells in the CSF was determined; averages ± SD are depicted ($n = 2–14$ mice/group). *B*, Composition of the LCMV-induced cellular infiltrate as a function of time. CXCR3-deficient and WT mice were infected intracerebrally with 10^3 LD_{50}, and on the indicated days, CSF was harvested and cells were stained with anti-CD8, anti-CD4, anti-Mac-1, and anti-B220 (B-cell marker) ($n = 4–5$/group).

Unimpaired leukocyte recruitment to CSF in intracerebral-infected CXCR3-deficient mice

To evaluate the capacity of CXCR3-deficient mononuclear cells to migrate from the blood into the LCMV-infected brain, we next compared the influx of cells into the CSF of virus-infected CXCR3-deficient and matched WT mice. As shown in Figure 4*A*, no statistically significant differences in the number of mononuclear cells contained in the CSF were revealed between the mouse strains on 5, 6, 7 or 9 dpi, although a trend toward a slight delay in cellular influx was noted in CXCR3-deficient mice. By 14 and 21 dpi, all the infected WT mice had died of $CD8^+$ T-cell-mediated immunopathology, whereas the majority of CXCR3-deficient mice survived despite a chronic meningeal inflammation. These findings indicate that the expression of CXCR3 is not pivotal for the overall recruitment of mononuclear cells to the CSF. Furthermore, when analyzing the phenotypic composition of the inflammatory cells in the CSF with regard to $CD4^+$ and $CD8^+$ T-cells, Mac-1^+ macrophages, and $B220^+$ B-cells, we saw no substantial differences between the two mouse strains (Fig. 4*B*). Thus, $CD8^+$ T-cells are the predominant cell type found in CSF of LCMV-infected mice, and together with macrophages, they make-up the majority (>90%) of the inflammatory cells present in both strains during the acute phase of the antiviral immune response. However, later in the infection (19–35 dpi), the surviving

CXCR3-deficient mice present a marked change in the cellular composition of the inflammatory exudate. Macrophages become less frequent, and the composition of the lymphocyte population changes: the percentage of $CD4^+$ T-cells increases to ~30–40% of all cells, whereas $CD8^+$ T-cells tend to become less frequent (45–55%), although still the dominant lymphocyte subset. Finally, the frequency of B-cells increases (up to 10% of infiltrating CSF cells) compared with what is found during the acute phase (Fig. 4*B*). This gradual shift in the composition of the inflammatory exudate is consistent with what we have previously observed in mice that, for various reasons, survive the acute phase of this infection (Christensen et al., 1995).

Comparison of cerebral mRNA expression in intracerebrally infected CXCR3-deficient and WT mice

To further investigate the importance of CXCR3 in establishing the T-cell-mediated inflammatory response in the brain of LCMV-infected mice, we analyzed for the presence of transcripts specific for cell subset markers and cytokines using RPA. CXCR3-deficient and WT mice were infected intracerebrally with LCMV, and on 3 dpi (innate phase) and 7 dpi (specific phase), transcript levels in the brain were quantified. Mice that had been sham injected with the same volume of PBS intracerebrally were included as a control for mRNA expression unrelated to viral infection (Fig. 5A-B). On 3 dpi, we did not observe any difference between WT and CXCR3-deficient mice. However, on 7 dpi, transcript levels for CD3, CD8, and IFN-γ might be lower in knock-outs than in WT mice: in some experiments, little or no difference was observed (data not shown), whereas in others a significant reduction could be found (Fig. 5*A*,*B*). In light of the observed kinetics of cell recruitment to the CSF (Fig. 4A), we interpret this spread to reflect that effector cell infiltration may be slightly delayed, but not abolished, in CXCR3-deficient mice; more outliers in the low range would account for the observed interexperimental variation. However, it is also clear that in the majority of CXCR3-deficient mice, the reduction in the number of effector $CD8^+$ T-cells present in the brain is limited (based on transcript levels twofold or less), and CXCR3 deficient mice survived despite chronic $CD8^+$ T-cell infiltration (Fig. 4*A*,*B*).

To see whether there should be a difference in the cerebral chemokine and chemokine receptor profile in the absence of CXCR3 expression, we evaluated chemokine and chemokine receptor transcription in the same mice as used in Figure 5, *A* and *B*. As shown in Figure 5, *C* and *D*, neither the composition nor the kinetics of chemokine and chemokine receptor gene expression was different in CXCR3-deficient mice compared with WT mice, except, of course, for the lack of CXCR3 expression. Thus, failure to express CXCR3 does not result in a changed pattern of activation of chemokine genes in the virus-infected brain, and the chemokine receptor profile remains essentially the same.

No accumulation of $CD8^+$ T-cells in the brain parenchyma of LCMV-infected CXCR3-deficient mice

The above results indicate that extravasation and overall influx of activated $CD8^+$ T-cells into the virus-infected CNS may be delayed, but not abolished, in CXCR3-deficient mice. This suggests that it is not merely the number of infiltrating $CD8^+$ T-cells but also their positioning that limits CNS immunopathology in these mice. To study this more directly, we evaluated the localization of $CD8^+$ T-cells through immunohistological analysis. CXCR3-deficient and WT mice were infected intracerebrally with LCMV and analyzed 7 dpi. The CXCR3-deficient mice were further evaluated on 14 and 21 dpi.

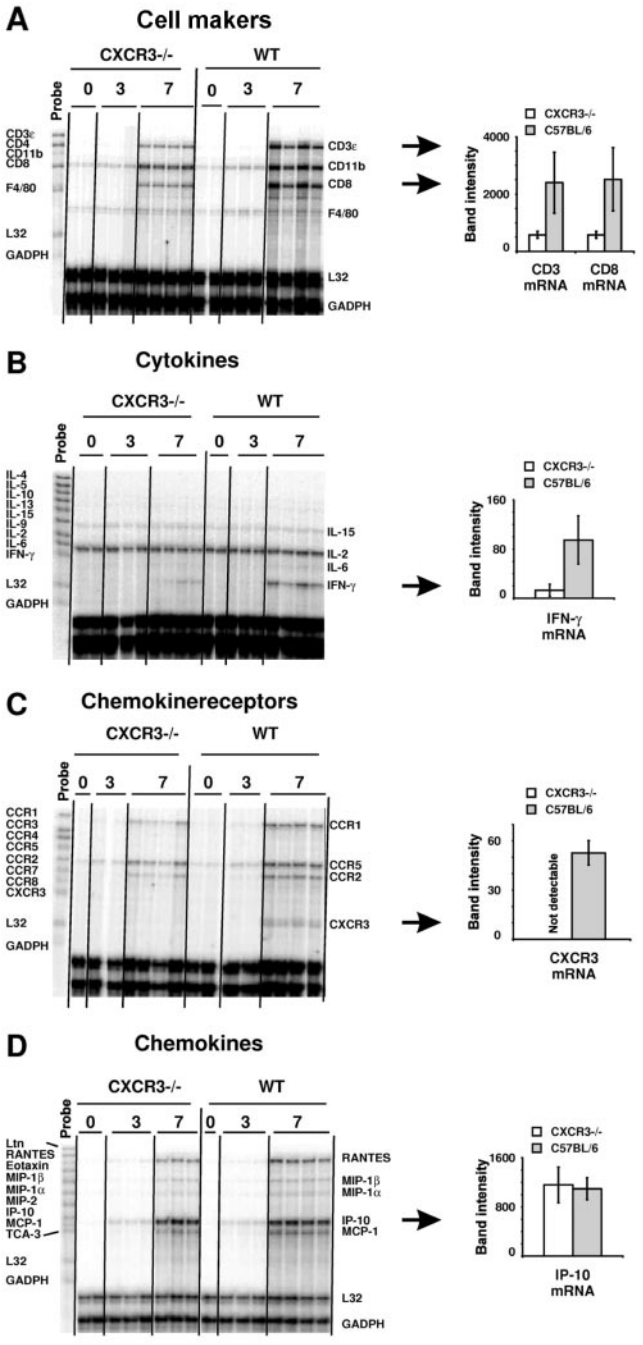

Figure 5. Comparison of cerebral mRNA expression after intracerebral LCMV infection. CXCR3-deficient and WT mice were infected intracerebrally with 10^3 LD_{50} of LCMV or injected with PBS (day 0 control). On the indicated days, total RNA was isolated from the brain of individual mice, and 20 μg was subjected to RPA analysis. Top lane, Expression of cell subset markers (*A*) and cytokines (*B*); bottom lane, expression of chemokines (*C*) and chemokine receptors (*D*).

At 7 dpi, WT animals presented clear signs of infection in terms of shivering, gait disturbances, and lachrymal secretion. At the microscopic level, the meninges exhibited prominent signs of inflammation as revealed by the presence of edema and multiple $CD8^+$ immunoreactive cells. $CD8^+$ cells were also seen in the choroid plexuses and brain regions nearby, suggesting that $CD8^+$ T-cells migrate from the ventricular system and further into the brain (Fig. 6*A*,*B*). The meningeal accumulation of $CD8^+$ cells was predominantly marked in many of the cisterns. In the brain

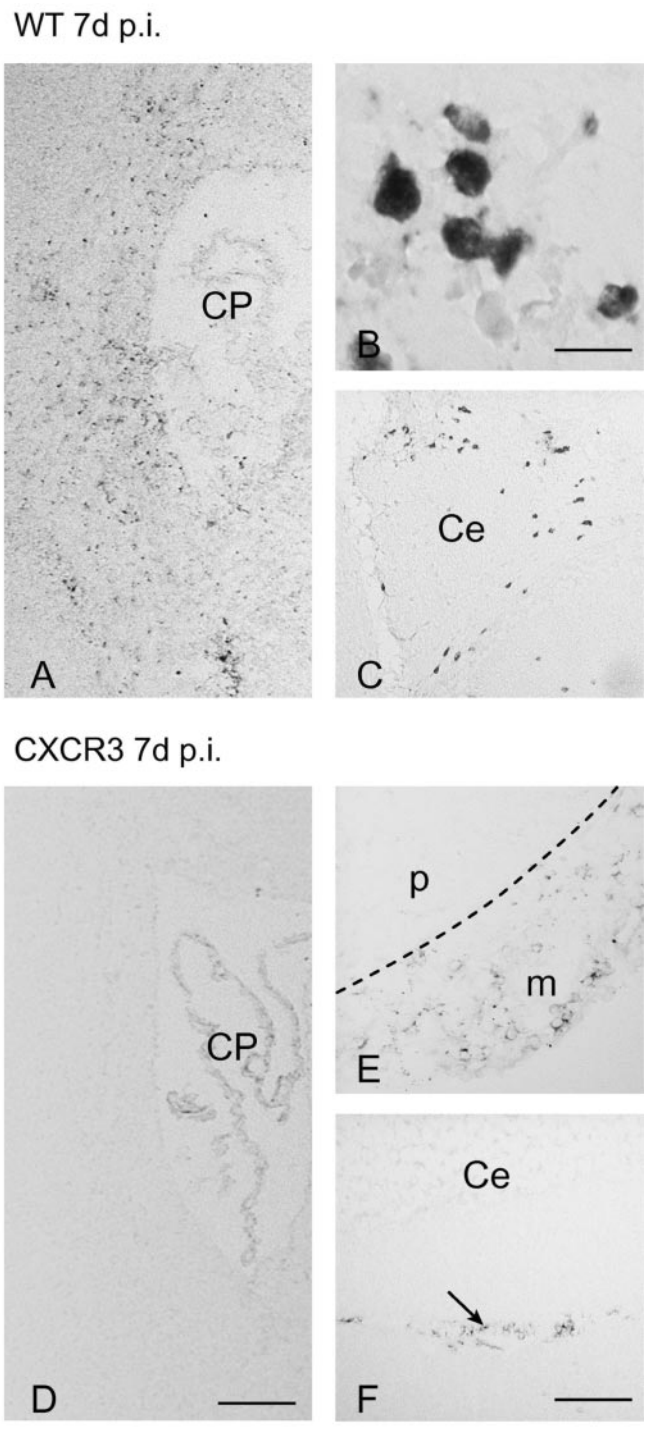

Figure 6. Failure of CD8$^+$ T-cells to infiltrate the brain parenchyma in CXCR3-deficient mice. Immunohistochemistry analysis of brain sections from WT and CXCR3-deficient mice infected intracerebrally with 10^3 LD_{50} of LCMV. *A–C*, WT mice examined 7 dpi. *A*, Section taken from the level of the lateral choroid plexus (CP). CD8$^+$ T-cells accumulate in brain regions near the ventricular system. *B*, CD8$^+$ T-cells from the brain parenchyma shown at high magnification. *C*, T-cell accumulation in the cerebellum (Ce). CD8$^+$ T-cells mainly occur in the white matter. *D–F*, CXCR3-deficient mice examined 7 dpi. *D*, Section taken at the level of the lateral ventricle containing the choroid plexus (CP). CD8$^+$ T-cells do not accumulate in the brain parenchyma. *E*, Section from the ventral part of the brain stem showing accumulation of CD8$^+$ T-cells in the meninges (m). The dashed line separates the meninges from the brain parenchyma (p), which is devoid of CD8$^+$ T-cells. *F*, Section from the hind brain. CD8$^+$ T-cells (arrow) localize to the meninges between the cerebellum (Ce) and the lower brain stem. Scale bars: *A*, *D* (in *D*), 200 μm; *B*,10 μm; *C*, *E*, *F* (in *F*), 100 μm.

Table 1. Reduced infiltration of CD8$^+$ T-cells into neural parenchyma of CXCR3-deficient mice infected intracerebrally with LCMV

	Days post infection	
	Day 7	Day 14
WT	20.40 ± 2.15[a]	No surviving
CXCR3 deficient	2.06 ± 0.42[b]	6.34 ± 0.94[c]

[a]Number of CD8$^+$ T-cells/150,000 μm^2 (average ± SD).
[b]Significant difference between WT and CXCR3-deficient mice on 7 dpi ($p < 0.01$).
[c]Significant difference between CXCR3-deficient mice on 7 and 14 dpi ($p < 0.01$).

parenchyma, the highest accumulation of T-cells was seen in white matter regions such as the corpus callosum, internal capsule, and the white matter of the cerebellum (Fig. 6*C*). Because most WT mice do not survive beyond 8 dpi, WT mice were not examined at later time points.

In contrast to WT mice, CXCR3-deficient mice were almost devoid of symptoms on 7 dpi. Microscopically, presence of CD8$^+$ cells was almost completely restricted to the meninges and choroid plexuses (Fig. 6*D–F*). In comparison with WT mice, it was not the impression that the number of CD8$^+$ cells infiltrating the meninges or accumulating in the choroid plexuses was reduced. However, the prominent appearance of CD8$^+$ cells in brain parenchymal regions near the ventricular surfaces seen in WT mice was not recapitulated in CXCR3-deficient mice analyzed at 7 dpi (Fig. 6*D–F*; Table 1). Hence, it was not possible to detect CD8$^+$ T-cells anywhere in the brain parenchyma, except for a bright appearance near the interpedunculate cistern of the mesencephalon.

To see whether the difference in the distribution of CD8$^+$ T-cells reflected a difference in localization of virus-infected cells, brain sections were also compared with regard to the distribution of virus-infected cells. Viral protein was detected in choroid plexus epithelial cells, cells of the meninges, and inflammatory cells of both genotypes (Fig. 7). The labeled inflammatory cells were observed diffusely around the surfaces of the ventricular system and in major white matter tracts such as the corpus callosum (Fig. 7*A*), internal and external capsules, and the pyramidal tract. The cellular labeling intensity obtained by the anti-LCMV antibody was indistinguishable when compared between WT and CXCR3-deficient mice (Fig. 7*D*,*E*). Thus, a difference in extent or distribution of virus-infected target cells could not explain the marked difference in localization of CD8$^+$ T-cells.

At later time points after infection, the distribution of CD8$^+$ cells in CXCR3-deficient mice differed from that observed at 7 dpi in that more CD8$^+$ T-cells had penetrated into the brain parenchyma (Table 1). However, compared with the pattern observed in WT mice examined at 7 dpi, the accumulation was substantially lower in the CXCR3-deficient mice examined at 14 dpi (Table 1) or 21 dpi (data not shown). This observation was also made clinically because the behavior of these CXCR3 mice was identical to CXCR3 mice examined at 7 dpi. Thus, fewer CD8$^+$ effector T-cells were seen to penetrate into the brain parenchyma in the absence of CXCR3 expression.

Restored susceptibility to LCMV-induced T-cell-mediated meningitis in CXCR3-deficient mice reconstituted with CXCR3$^+$ CD8$^+$ T-cells

If the high survival rate of CXCR3-deficient mice is the result of an impaired capacity of CXCR3$^-$ CD8$^+$ effector T-cells to reach critical target areas in the brain, then adoptive transfer of CXCR3$^+$ CD8$^+$ T-cells to these mice should restore the susceptibility to intracerebral infection. To test this prediction, CXCR3-

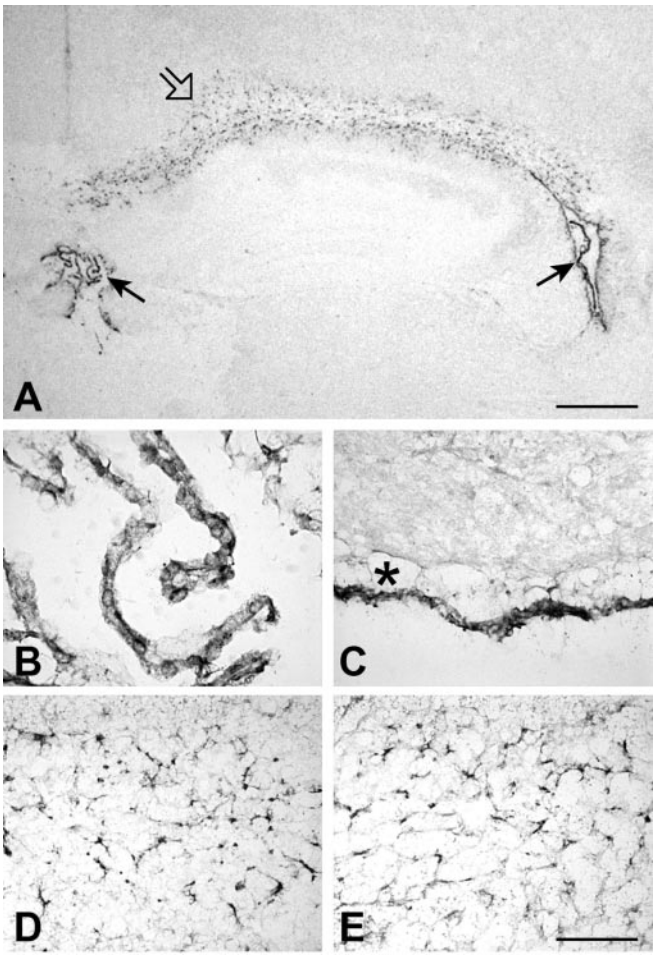

Figure 7. Immunohistochemical detection of LCMV virus in CXCR3-deficient (*A–D*) and WT (*E*) mice at 7 dpi. *A*, Section of the forebrain showing viral infection of choroid plexuses of the lateral and third ventricles (arrows) and inflammatory cells dispersed within the corpus callosum (open arrow). *B*, Labeling of choroid plexus epithelial cells shown at higher magnification. *C*, Section from the ventral part of the mesencephalon showing labeling of meninges. The subarachnoid space identified by an asterisk separates the inflamed meninges from unlabeled brain parenchyma. *D*, *E*, Sections of the corpus callosum of the CXCR3-deficient (*D*) and WT (*E*) mice. The number and distribution of inflammatory cells between the different mice are indistinguishable. Scale bars: *A*, 300 μm; *B–E* (in *E*), 100 μm.

deficient mice were again infected intracerebrally with LCMV, and 3 d later, part of the mice were given a low number (3×10^6) of splenocytes from naive mice transgenic for an LCMV-specific, class I-restricted TCR. Another group of mice were given the same number of TCR transgenic splenocytes depleted of $CD8^+$ T-cells. The mortality of these groups and an untransplanted control group was registered over the next 2 weeks. As shown in Figure 8, all CXCR3-deficient mice reconstituted with $CD8^+$ replete $CXCR3^+$ splenocytes died within 9 d of infection ($p < 0.001$ vs untransplanted mice; Mantel–Cox test), matching the pattern normally seen with similarly infected WT mice (Fig. 2). In contrast, only approximately one-third of CXCR3-deficient mice reconstituted with $CXCR3^+$ splenocytes depleted of $CD8^+$ cells died from the infection; this is significantly fewer than after transfer of $CD8^+$ replete cells ($p < 0.001$; Mantel–Cox test) and not significantly more than observed with untransplanted CXCR3-deficient mice ($p > 0.09$). Taken together, these findings underscore that the relative resistance of CXCR3-deficient mice does not reflect an absence of critical target elements within the CNS and strongly support the hypothesis that lack of $CXCR3^+$ $CD8^+$ T-cells constitutes the most important factor preventing a lethal outcome of intracerebral infection with LCMV in CXCR3-deficient mice.

Unimpaired T-cell-mediated inflammation in the virus-infected footpad

Finally, to see whether absence of CXCR3 generally suppressed $CD8^+$ T-cell-mediated inflammation, mice were infected in the footpad, and the induced swelling was measured (Fig. 9). Similar to LCMV-induced CNS disease, the virus-induced footpad swelling primarily reflects virus-specific $CD8^+$ T-cell-mediated inflammation (Christensen et al., 1994). However, unlike the situation after intracerebral infection, little difference in T-cell-mediated inflammation of the foot was observed.

Discussion

The major evolutionary importance of $CD8^+$ effector T-cells lies in their ability to eliminate virus-infected cells. Because viruses generally are rapidly replicating agents that may be found in any organ site, varying with the specific tropism of the particular virus, it is crucial for the host to generate a population of effector cells with the capacity to rapidly become focused at any site of active virus replication. After proper activation, T-cells downregulate chemokine receptors responsible for homing to secondary lymphoid organs (i.e., CCR7) and instead upregulate receptors for inflammatory chemokines; in the case of type 1 (IFN-γ producing; Th1/Tc1) effector T-cells, which are the relevant effector T-cell type in antiviral immunity (Cerwenka et al., 1999), expression of the receptors CCR5 and CXCR3 is characteristic (Sallusto et al., 2000). In a previous study, we focused our attention on the role of CCR5 in antiviral immunity because it is a major coreceptor for human immunodeficiency virus and thus an obvious target for pharmacological intervention. However, so far analysis regarding the biological function of this receptor indicates that expression of CCR5 is not critical for T-cell-mediated antiviral immunity (Nansen et al., 2002), and because CXCR3 is another prototypic chemokine receptor of type 1 T-cells, we found it pertinent to determine the importance of this inflammatory chemokine receptor in antiviral immunity.

In the present study, we used intracerebral infection with LCMV as our model system.

This is a unique model well suited for the study of T-cell-mediated antiviral immunity because the kinetics of the response and the effector mechanisms are extremely well defined (Doherty et al., 1990). Most importantly, because the virus by itself is noncytolytic, a fatal outcome of intracerebral infection is directly related to efficient delivery of cytolytic $CD8^+$ T-cells to areas of virus infection within the CNS (Kagi et al., 1994).

Using this system, a number of observations have been obtained that all point to a pivotal role for CXCR3 in controlling the migration of antiviral effector $CD8^+$ T-cells to sites of viral replication within the CNS. First, transcript levels for CXCR3 are upregulated in LCMV-infected organs of immunocompetent mice (Lindow et al., 2003). Second, CXCR3 is expressed on antigen-primed $CD8^+$ T-cells, including those generated in the context of viral infection (Fig. 1). Third, mRNA levels for CXCL10 are rapidly upregulated in virus-infected organs, including the CNS (Asensio et al., 1999; Nansen et al., 2000). Fourth, *in vitro* CXCL10 functions as a chemoattractant of relevant effector cells (i.e., activated $CD8^+$ T-cells and monocyte/macrophages) (Frigerio et al., 2002; Lindow et al., 2003), and this requires expression of CXCR3 (present study). Most important, mice deficient in CXCR3 expression infected intracerebrally with LCMV

are relatively resistant to the virus-induced CD8$^+$ T-cell-mediated meningitis, which invariably kills similarly infected WT mice (Fig. 2). Whereas the latter observation in itself does not prove that CXCR3 is required during the effector phase of the immune response, additional experimental evidence strongly points to that interpretation.

Thus, with regard to the induction of the antiviral T-cell response, our analysis did not reveal important immunological abnormalities in the absence of the CXCR3 receptor. Thus, the generation of CD8$^+$ effector T-cells was not impaired as measured by CD8$^+$ T-cell expansion (Fig. 3), upregulation of adhesion molecules, and chemokine receptor CCR5 (data not shown) together with secretion of proinflammatory cytokines *ex vivo* (Fig. 3). Furthermore, we found that *in vivo*-activated CXCR3-deficient splenocytes had not lost their ability to migrate toward CCL3 in an *in vitro* migration assay (data not shown). However, although these results fail to demonstrate a role for CXCR3 in the generation of an adaptive immune responses in the LCMV model, others have found that CXCR3 and CXCL10 signaling somewhat enhances the generation of effector cells after other types of immunization (Luster et al., 1985; Hancock et al., 2000). We ascribe this discrepancy to the fact that LCMV injected intracerebrally very readily accesses the bloodstream (~90% of the inoculum is believed to go intravenously) and thus reaches the secondary lymphoid organs without any requirement for mobilization of antigen-presenting cells. Perhaps also the fact that LCMV actively replicates in lymph nodes and spleen may further minimize any requirement for CXCR3 expression during the induction phase of the immune response.

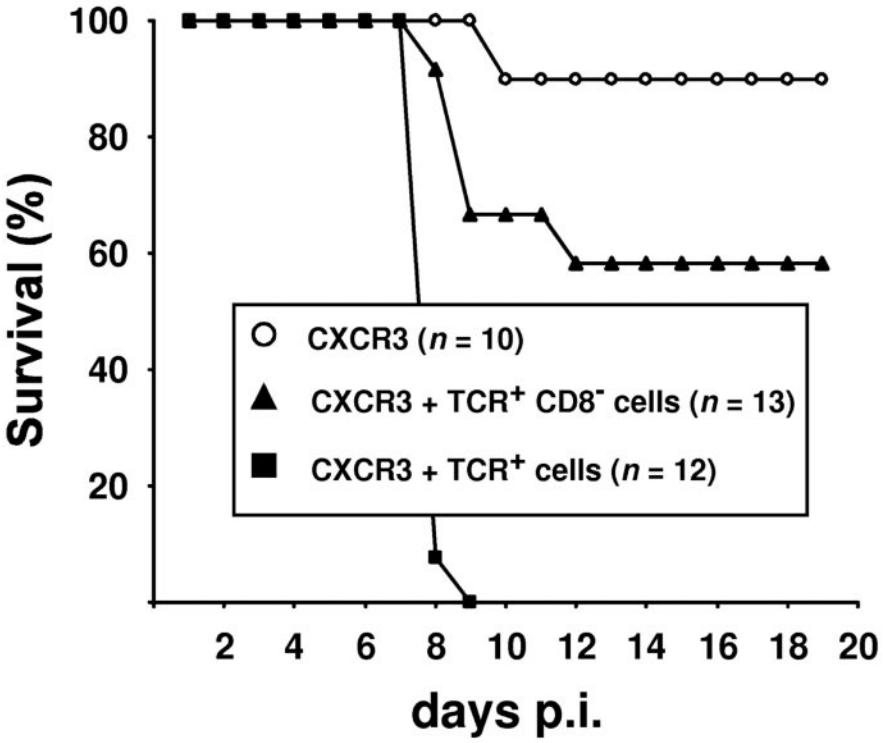

Figure 8. CXCR3$^+$ CD8$^+$ T-cells restore susceptibility to LCMV-induced meningitis in CXCR3-deficient mice. CXCR3-deficient mice were infected intracerebrally with 10^3 LD_{50} of LCMV, and 3 d later, part of the mice were transfused with 3×10^6 splenocytes from naive TCR transgenic mice expressing a TCR specific for LCMV gp33-41. Another group received the same number of transgenic splenocytes depleted of CD8$^+$ T-cells (validated by flow cytometry). The mortality of these groups and a group of untransplanted virus-infected CXCR3-deficient mice was registered ($n = 10–13$ mice/group).

To directly evaluate the ability of inflammatory cells to reach the virus-infected CNS in the absence of CXCR3 signaling, we studied the inflammatory response in the brain. Comparing chemokine gene expression patterns in the brain of LCMV-infected CXCR3-deficient and WT mice, we saw no change in the chemokine profile as a result of CXCR3 deficiency (Fig. 5*C*). In addition, both quantitative and qualitative analysis of the inflammatory cells present in the CSF of intracerebrally infected mice failed to reveal substantial differences between CXCR3-deficient and WT mice (Fig. 4); a trend toward a delay in influx was noted, but this was not statistically significant. When transcripts directly related to the influx of inflammatory cells were studied (Fig. 5*A*,*B*), we saw a similar spread in the results from CXCR3-deficient mice, which in some cases matched wild types, whereas in others a reduced response was observed. We interpret this variation to reflect a slight impairment in effector cell recruitment to the virus-infected CNS in CXCR3-deficient mice. However, as indicated by the CSF data, peak levels are likely to be only minimally reduced, and the majority of CXCR3-deficient mice survive intracerebrally challenge despite chronic CD8$^+$ T-cell infiltration of the meninges. Together, the above observations therefore point to the interpretation that it is not simply the number of infiltrating effector CD8$^+$ T-cells that limits the immunopathology of LCMV-infected CXCR3-deficient mice. This view was convincingly supported by immunohistological analysis, revealing the presence of CD8$^+$ cells in the brain parenchyma of WT mice but not of CXCR3-deficient mice (Fig. 6; Table 1), despite similar localization of virus-infected target cells (Fig. 7). Consistent with a role for CXCR3 in directing the positioning of CD8$^+$ T-cells within the virus-infected brain, a recent study using *in situ* hybridization to analyze the localization of CXCL10 transcripts

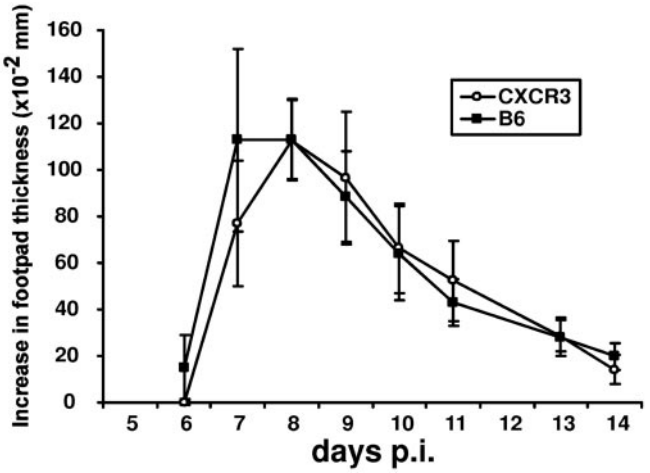

Figure 9. Unimpaired LCMV-induced T-cell-mediated inflammation in the footpad. LCMV-induced footpad swelling was assessed in mice infected locally in the right hind footpad with 200 pfu of LCMV. Virus-specific swelling was calculated as the difference in thickness of the infected right and the uninfected left hind foot. One of two similar experiments is presented; averages ± SD are depicted ($n = 5$ mice/group).

in the LCMV-infected brain revealed the presence of CXCL10-producing cells in the brain parenchyma including the cerebellum and subcortical regions of the brain (Asensio et al., 1999); these are exactly the same areas in which we found $CD8^+$ T-cells in WT mice but not in CXCR3-deficient mice (Fig. 6). Thus, the presence of CXCL10 in the brain parenchyma could facilitate the recruitment of virus-specific $CXCR3^+$ $CD8^+$ T-cells into these critical areas. Finally, strongly supporting a role for $CXCR3^+$ effector T-cells, we could abrogate the resistance to LCMV-induced disease in CXCR3-deficient mice by reconstituting with $CXCR3^+$ $CD8^+$ T-cells (Fig. 8). Taken together, these findings strongly indicate that although CXCR3 may be redundant for the cellular interactions required for extravasation and crossing of the blood–CSF barrier (i.e., the almost unimpaired recruitment of inflammatory cells to CSF), CXCR3 signaling plays a central role for efficient migration of $CD8^+$ effector T-cells to critical areas deeper inside the virus-infected CNS.

The implications of these findings are twofold. First, regarding LCMV-induced meningitis, the present results provide important new insight into the pathophysiology of this disease. The presently most favored hypothesis regarding what causes a fatal outcome is that virus-specific $CD8^+$ T-cells kills virus-infected cells in the meninges and choroid plexus in a perforin-dependent manner (Kagi et al., 1994). However, given that alleviation of clinical disease in CXCR3-deficient mice correlates with a failure of the effector T-cells to penetrate deeper into the CNS, it may actually be in these sites that one should search for the cellular disturbances that are responsible for a fatal outcome.

More important, our study provides new information regarding the molecular interactions that control T-cell migration and surveillance within the CNS, and because Th1 and Tc1 cells have a similar pattern of chemokine receptor expression, our findings may have important implications for the treatment of neuroimmunoinflammatory diseases in general. Thus, it would appear likely that MS and similar diseases might be inhibited by targeting of CXCR3. Furthermore, the fact that only certain facets of T-cell-mediated immunity (i.e., the unimpaired inflammatory response in the virus-infected foot) (Fig. 9) requires CXCR3 suggests that the design of CXCR3 antagonists would provide the means for more accurate intervention, which is likely to minimize the side effects associated with conventional immunosuppressive treatment.

References

Andersson EC, Christensen JP, Marker O, Thomsen AR (1994) Changes in cell adhesion molecule expression on T cells associated with systemic virus infection. J Immunol 152:1237–1245.

Andreasen SO, Christensen JP, Marker O, Thomsen AR (1999) Virus-induced non-specific signals cause cell cycle progression of primed CD8(+) T cells but do not induce cell differentiation. Int Immunol 11:1463–1473.

Asensio VC, Campbell IL (1997) Chemokine gene expression in the brains of mice with lymphocytic choriomeningitis. J Virol 71:7832–7840.

Asensio VC, Kincaid C, Campbell IL (1999) Chemokines and the inflammatory response to viral infection in the central nervous system with a focus on lymphocytic choriomeningitis virus. J Neurovirol 5:65–75.

Balashov KE, Rottman JB, Weiner HL, Hancock WW (1999) CCR5(+) and CXCR3(+) T cells are increased in multiple sclerosis and their ligands MIP-1alpha and IP-10 are expressed in demyelinating brain lesions. Proc Natl Acad Sci USA 96:6873–6878.

Battegay M, Cooper S, Althage A, Banziger J, Hengartner H, Zinkernagel RM (1991) Quantification of lymphocytic choriomeningitis virus with an immunological focus assay in 24- or 96-well plates. J Virol Methods [Erratum (1991) 35:115 and (1992) 38:263] 33:191–198.

Ceredig R, Allan JE, Tabi Z, Lynch F, Doherty PC (1987) Phenotypic analysis of the inflammatory exudate in murine lymphocytic choriomeningitis. J Exp Med 165:1539–1551.

Cerwenka A, Morgan TM, Harmsen AG, Dutton RW (1999) Migration kinetics and final destination of type 1 and type 2 CD8 effector cells predict protection against pulmonary virus infection. J Exp Med 189:423–434.

Christensen JP, Marker O, Thomsen AR (1994) The role of CD4+ T cells in cell-mediated immunity to LCMV: studies in MHC class I and class II deficient mice. Scand J Immunol 40:373–382.

Christensen JP, Andersson EC, Scheynius A, Marker O, Thomsen AR (1995) Alpha 4 integrin directs virus-activated CD8+ T cells to sites of infection. J Immunol 154:5293–5301.

Doherty PC, Allan JE, Lynch F, Ceredig R (1990) Dissection of an inflammatory process induced by CD8+ T cells. Immunol Today 11:55–59.

Dufour JH, Dziejman M, Liu MT, Leung JH, Lane TE, Luster AD (2002) IFN-gamma-inducible protein 10 (IP-10; CXCL10)-deficient mice reveal a role for IP-10 in effector T cell generation and trafficking. J Immunol 168:3195–3204.

Fife BT, Kennedy KJ, Paniagua MC, Lukacs NW, Kunkel SL, Luster AD, Karpus WJ (2001) CXCL10 (IFN-gamma-inducible protein-10) control of encephalitogenic CD4+ T cell accumulation in the central nervous system during experimental autoimmune encephalomyelitis. J Immunol 166:7617–7624.

Franciotta D, Martino G, Zardini E, Furlan R, Bergamaschi R, Andreoni L, Cosi V (2001) Serum and CSF levels of MCP-1 and IP-10 in multiple sclerosis patients with acute and stable disease and undergoing immunomodulatory therapies. J Neuroimmunol 115:192–198.

Frigerio S, Junt T, Lu B, Gerard C, Zumsteg U, Hollander GA, Piali L (2002) Beta cells are responsible for CXCR3-mediated T-cell infiltration in insulitis. Nat Med 8:1414–1420.

Hancock WW, Lu B, Gao W, Csizmadia V, Faia K, King JA, Smiley ST, Ling M, Gerard NP, Gerard C (2000) Requirement of the chemokine receptor CXCR3 for acute allograft rejection. J Exp Med 192:1515–1520.

Hickey WF (2001) Basic principles of immunological surveillance of the normal central nervous system. Glia 36:118–124.

Kagi D, Ledermann B, Burki K, Seiler P, Odermatt B, Olsen KJ, Podack ER, Zinkernagel RM, Hengartner H (1994) Cytotoxicity mediated by T cells and natural killer cells is greatly impaired in perforin-deficient mice. Nature 369:31–37.

Karpus WJ, Ransohoff RM (1998) Chemokine regulation of experimental autoimmune encephalomyelitis: temporal and spatial expression patterns govern disease pathogenesis. J Immunol 161:2667–2671.

Kolb SA, Sporer B, Lahrtz F, Koedel U, Pfister HW, Fontana A (1999) Identification of a T cell chemotactic factor in the cerebrospinal fluid of HIV-1-infected individuals as interferon-gamma inducible protein 10. J Neuroimmunol 93:172–181.

Lahrtz F, Piali L, Nadal D, Pfister HW, Spanaus KS, Baggiolini M, Fontana A (1997) Chemotactic activity on mononuclear cells in the cerebrospinal fluid of patients with viral meningitis is mediated by interferon-gamma inducible protein-10 and monocyte chemotactic protein-1. Eur J Immunol 27:2484–2489.

Lindow M, Nansen A, Bartholdy C, Stryhn A, Hansen NJV, Boesen TP, Wells TNC, Schwartz TW, Thomsen AR (2003) The virus-encoded chemokine vMIP-II inhibits virus-induced Tc1-driven inflammation. J Virol 77:7393–7400.

Liu MT, Chen BP, Oertel P, Buchmeier MJ, Armstrong D, Hamilton TA, Lane TE (2000) The T cell chemoattractant IFN-inducible protein 10 is essential in host defense against viral-induced neurologic disease. J Immunol 165:2327–2330.

Liu MT, Keirstead HS, Lane TE (2001) Neutralization of the chemokine CXCL10 reduces inflammatory cell invasion and demyelination and improves neurological function in a viral model of multiple sclerosis. J Immunol 167:4091–4097.

Loetscher M, Gerber B, Loetscher P, Jones SA, Piali L, Clark-Lewis I, Baggiolini M, Moser B (1996) Chemokine receptor specific for IP10 and mig: structure, function, and expression in activated T-lymphocytes. J Exp Med 184:963–969.

Lowenstein PR (2002) Immunology of viral-vector-mediated gene transfer into the brain: an evolutionary and developmental perspective. Trends Immunol 23:23–30.

Luster AD, Unkeless JC, Ravetch JV (1985) Gamma-interferon transcriptionally regulates an early-response gene containing homology to platelet proteins. Nature 315:672–676.

Madsen AN, Nansen A, Christensen JP, Thomsen AR (2003) Role of macrophage inflammatory protein-1alpha in T-cell-mediated immunity to viral infection. J Virol 77:12378–12384.

Nansen A, Marker O, Bartholdy C, Thomsen AR (2000) CCR2+ and CCR5+ CD8+ T cells increase during viral infection and migrate to sites of infection. Eur J Immunol 30:1797–1806.

Nansen A, Christensen JP, Andreasen SO, Bartholdy C, Christensen JE, Thomsen AR (2002) The role of CC chemokine receptor 5 in antiviral immunity. Blood 99:1237–1245.

Odermatt B, Eppler M, Leist TP, Hengartner H, Zinkernagel RM (1991) Virus-triggered acquired immunodeficiency by cytotoxic T-cell-dependent destruction of antigen-presenting cells and lymph follicle structure. Proc Natl Acad Sci USA 88:8252–8256.

Pircher H, Burki K, Lang R, Hengartner H, Zinkernagel RM (1989) Tolerance induction in double specific T-cell receptor transgenic mice varies with antigen. Nature 342:559–561.

Ransohoff RM (1999) Mechanisms of inflammation in MS tissue: adhesion molecules and chemokines. J Neuroimmunol 98:57–68.

Sallusto F, Mackay CR, Lanzavecchia A (2000) The role of chemokine receptors in primary, effector, and memory immune responses. Annu Rev Immunol 18:593–620.

Simpson JE, Newcombe J, Cuzner ML, Woodroofe MN (2000) Expression of the interferon-gamma-inducible chemokines IP-10 and Mig and their receptor, CXCR3, in multiple sclerosis lesions. Neuropathol Appl Neurobiol 26:133–142.

Sorensen TL, Tani M, Jensen J, Pierce V, Lucchinetti C, Folcik VA, Qin S, Rottman J, Sellebjerg F, Strieter RM, Frederiksen JL, Ransohoff RM (1999) Expression of specific chemokines and chemokine receptors in the central nervous system of multiple sclerosis patients. J Clin Invest 103:807–815.

Sorensen TL, Trebst C, Kivisakk P, Klaege KL, Majmudar A, Ravid R, Lassmann H, Olsen DB, Strieter RM, Ransohoff RM, Sellebjerg F (2002) Multiple sclerosis: a study of CXCL10 and CXCR3 co-localization in the inflamed central nervous system. J Neuroimmunol 127:59–68.

Thomsen AR, Marker O (1989) MHC and non-MHC genes regulate elimination of lymphocytic choriomeningitis virus and antiviral cytotoxic T lymphocyte and delayed-type hypersensitivity mediating T lymphocyte activity in parallel. J Immunol 142:1333–1341.

Trebst C, Ransohoff RM (2001) Investigating chemokines and chemokine receptors in patients with multiple sclerosis: opportunities and challenges. Arch Neurol 58:1975–1980.

Weng Y, Siciliano SJ, Waldburger KE, Sirotina-Meisher A, Staruch MJ, Daugherty BL, Gould SL, Springer MS, DeMartino JA (1998) Binding and functional properties of recombinant and endogenous CXCR3 chemokine receptors. J Biol Chem 273:18288–18291.

Zhang GX, Baker CM, Kolson DL, Rostami AM (2000) Chemokines and chemokine receptors in the pathogenesis of multiple sclerosis. Mult Scler 6:3–13.